Journal of Power Sources 244 (2013) 252–258

Contents lists available at SciVerse ScienceDirect

Journal of Power Sources

journal homepage: www.elsevier.com/locate/jpowsour

Quantification of lithium in LIB electrodes with glow discharge optical emission spectroscopy (GD-OES)

Hikari Takahara [a,*], Masahiro Shikano [b], Hironori Kobayashi [b]

[a] Rigaku Corporation, 14-8 Akaoji-cho, Takatsuki, Osaka 569-1146, Japan
[b] National Institute of Advanced Industrial Science and Technology (AIST), 1-8-31, Midorigaoka, Ikeda, Osaka 563-8577, Japan

HIGHLIGHTS

- GD-OES was applied to quantification of Li in LIB electrodes.
- The samples were NCM and hard carbon based electrodes with SOC 0–100%.
- Depth profiles were successfully obtained from the surface to the current collector.
- Li intensities from GD-OES were correlated with the Li components by ICP-MS.

ARTICLE INFO

Article history:
Received 5 November 2012
Received in revised form
7 January 2013
Accepted 17 January 2013
Available online 28 January 2013

Keywords:
GD-OES
Depth profiling
Quantification analysis of lithium
LIB electrode analysis

ABSTRACT

Glow discharge optical emission spectroscopy (GD-OES) was applied to quantification of Li in both positive and negative electrodes. Depth profiles of $Li_{1.03}Ni_{0.32}Co_{0.33}Mn_{0.32}O_2$ (NCM) and hard carbon based electrodes in the range of state of charge (SOC) 0–100% were measured throughout from the surface to the current collector within a few hours. The flat crater shapes, although slightly concave at the edge for NCM, suggested a good depth resolution in the profiles. The sample surfaces sputtered during the GD-OES measurement were smooth in SEM observation, suggesting that remarkable preferential sputtering of the composite materials did not occur. The Li intensities obtained from GD-OES were correlated with the Li components determined using ICP-MS for both positive and negative electrode samples. The correlation coefficients of the linear relationship were improved by considering intensity ratio of Li to the matrix element, Li/Co and Li/C for NCM and hard carbon electrodes, respectively, to correct the sputtering rate variation of samples. These results confirm that GD-OES is a potential technique for quantitative analysis of Li in the electrodes.

1. Introduction

Lithium ion battery (LIB) has become an indispensable technology for portable electronic devices for the last two decades. Recently, the demands for LIB in wider applications such as energy vehicles and stationary storage systems are drastically increasing, so that many researches have been studied to improve its energy density, long-term stability, safety, and so on. To understand the fundamental behavior of the material in the electrochemical reaction is essential for the further development of LIB. Especially, characterization of lithium in the electrodes is crucial, because the behaviors of lithium such as reversible lithium in the electrodes and irreversible lithium consumed in solid electrolyte interphase (SEI) are the keys to influence the cell performance. Conventional analysis techniques such as X-ray diffraction (XRD), X-ray fluorescence (XRF), and electron probe micro analyzer (EPMA) are insufficient to characterize Li. X-ray photoelectron spectroscopy (XPS) [1–3], and nuclear magnetic resonance (NMR) [4–6], and scanning transmission electron energy loss (STEM-EELS) [7] have been well accepted for characterizing Li in the electrode so far.

Glow discharge optical emission spectroscopy (GD-OES) is an elemental analysis and a direct in-depth analysis technique for a bulk solid and thin film. Its equipment is furnished with a grim type glow discharge lump, where a sample is mounted facing as a cathode [8]. When argon is introduced into the source with low pressure (a few hundreds Pa) and a high voltage (500–1000 V) is applied to the cathode, electrical discharge plasma generates between the electrodes. The sample is atomized and excited in the

* Corresponding author. X-ray Analysis Division, Rigaku Corporation, 14-8, Akaoji-cho, Takatsuki, Osaka 569-1146, Japan. Tel.: +81 72 693 6813; fax: +81 72 694 6500.
E-mail address: hikari@rigaku.co.jp (H. Takahara).

0378-7753/$ – see front matter © 2013 Elsevier B.V. All rights reserved.
http://dx.doi.org/10.1016/j.jpowsour.2013.01.109

plasma discharge away from sample surface, as is cathodic sputtering of the sample. At the same time the characteristic emissions by the excited atoms are generated in plasma, which enables us optical elemental analysis. The aperture of the anode in the glow discharge lump is typically a few mm in diameter, which decides the measurement spot size. A typical sputtering rate is around 1 μm min^{-1} for stainless steel samples for example. GD-OES was previously utilized in steel and metal-plating industries for the trace elemental analysis and the depth profiling with direct current (dc) potential. Furthermore it has broaden to microelectronics field such as semiconductors, thin films, glasses and polymers in the benefit of the radio frequency (rf) potential which enables sputtering either conductive or non-conductive material because of the self-bias potential [9]. Also in the advanced field of lithium ion battery, the depth profiling of positive electrodes was attempted by rf-GD-OES [10] The lithium composition is evaluated from surface to the interface of the current collector totally for degraded $LiNi_{0.8}Co_{0.15}Al_{0.05}O_2$ electrodes with various states of charge (SOCs). The results show that the distributions of lithium are uniform in the degraded electrodes and that lithium compositions obtained by GD-OES well agree with those from induced coupled plasma-mass spectroscopy (ICP-MS). GD-OES is proposed as a potential analysis technique for depth profiling and quantification of Li in LIB electrode. On the basis of the proceeding study, we had objects to investigate the potential of GD-OES analysis in positive electrodes in detail and expand it to carbon negative electrodes. In the present study, the quantification of Li in both positive and negative electrodes was aimed using GD-OES technique. The $Li_{1.03}Ni_{0.32}Co_{0.33}Mn_{0.32}O_2$ (NCM) and hard carbon based batteries [11,12] were adjusted to the range of SOC 0–100% after pre-determined cycling, and the both electrode samples were measured with GD-OES. The sample surfaces sputtered in GD-OES measurement were investigated with scanning electron microscope (SEM) and XPS. The correlation between Li intensities obtained from GD-OES and Li components determined by ICP-MS was confirmed for the positive and negative electrode samples.

2. Experimental

$Li_{1.03}Ni_{0.32}Co_{0.33}Mn_{0.32}O_2$ (NCM) powder, provided by Toda Kogyo, was used as the positive electrode material [11]. The slurry consisting of 90% active material, 6% acetylene black, and 4% poly(vinylidene difluoride) (PVdF) was prepared by mixing in N-methyl-2-pyrrolidone (NMP) solvent and coated onto both sides of Al current collector. The loading and the thickness were 9.5 mg cm^{-2} and 31 μm on either side. Hard carbon powder was provided by Kureha for the negative electrode material. The negative electrode was prepared by casting the slurry consisting of 90.5% active material and 9.5% PVdF binder onto both sides of Cu current collector. The loading and the thickness were 3.8 mg cm^{-2} and 29 μm on either side. The cylindrical cells were assembled with the positive and negative electrodes, polymer separator (Asahi-Kasei Chemicals), and 1 mol dm^{-3} $LiPF_6$ in ethylene carbonate–diethyl carbonate electrolyte (EC:DMC, 1:2 in volume, Toyama − Chemical) in an Ar-filled glove box. Charge–discharge cycles were carried out for the cells at 3.0 and 4.3 V in cut-off voltages under 1 C in current rate at 25 °C. After the predetermined cycles, the SOCs of the cells were set to 0, 25, 50, 75, and 100% by a constant current charge with C/3 current rate. Here the current rate was defined to the NCM positive electrode. The cells adjusted to the various SOCs were disassembled and the obtained electrodes were rinsed with dimethyl carbonate (DMC) in an Ar-filled grove box and dried in vacuum.

GD-OES measurement was performed with GDA750 (Rigaku/Spectruma) for the positive and negative electrode samples. The samples were transferred to the apparatus using an experimental vessel without exposing to the air. Argon gas was employed for a discharging gas. Radio frequency power and pulsed glow discharge were applied with 500 V (or 20 W) electric voltage (or power) and 200 Pa gas pressure. The analyzed spot size was 4 mm in diameter for positive electrode samples. Alternative spot size of 2.5 mm was taken for negative electrode samples to gain the sputtering rate, because the sputtering rate of carbon electrode was several tens times lower than that of positive electrode samples. The lower sputtering rate of negative electrode could be explained from a factor of elemental sputtering yield, which is defined as the ratio between the number of atoms sputtered from the surface and the number of incident ion (Ar^+ in this measurement). The sputtering yield of C is very low; 0.12 atoms/ion toward 1.0 atoms/ion for Fe, at 400 eV Ar ions [14], whereas those of Mn, Co, and Ni were 0.8–1.3 atoms/ion at 400 eV Ar ions [14]. The following elements and their emission lines are applied in this study; H (121.57 nm), Li (610.41 or 670.78 nm), C (156.14 nm), O (130.22 nm), Al (396.15 nm), Mn (403.45 nm), Co (345.35 nm), Ni (341.48 nm), and Cu (219.22 nm). SEM imaging and XPS surface characterization were performed for the electrode samples before and after GD-OES measurement. The SEM micrographs were taken with 15 kV accelerating voltage (JSM 5500 LV; JEOL). XPS data were collected with Al Kα radiation source operated at 46.95 eV and an applied power of 25 W (PHI 5000 VersaProbe; Ulvac-Phi). The energies associated with each spectrum were calibrated to the C1s (284.6 eV), which is assigned mainly to C–C of acetylene black and hard carbon in the composite electrode. Besides the GD-OES measurement, the Li contents in the sample electrodes were determined by ICP-MS analysis (Table 1).

3. Result and discussion

3.1. GD-OES measurement of positive electrode samples

Fig. 1 shows a depth profile of an NCM electrode sample with 0% SOC obtained from GD-OES measurement. The intensities of Li, Mn, Ni, Co, O, C, H and Al are plotted as a function of the sputtering time instead of the distance from the surface. The NCM active material contributes with Li, Mn, Ni, Co and O, whereas the acetylene black and PVdF binder contribute with C and H. The sputtering pierced the electrode layer with 31 μm thickness and reached the Al current collector after 2600 s, which is reflected by a rapid increase of the Al intensity. The intensities of Li, Mn, Ni, Co, and O are almost constant in the whole region. Fig. 2(a) shows a crater shape for NCM sample with 100% SOC after 2000 s of measurement. The sputtering proceeded to about 25 μm depth from surface. The crater presents a smooth bottom whereas slightly concave at the edge, which allows depth profiling with good depth resolution [13]. In order to demonstrate the impact of sputtering for the NCM electrodes, SEM observation was performed. Fig. 2(b) and (c) shows SEM micrographs for the sample with 100% SOC, before and after 2000 s of measurement respectively. The surface features after 60 s and 600 s of measurement were similar to after 2000 s (not shown). It seems

Table 1
Li compositions determined by ICP-MS for NCM and hard carbon electrodes with various SOC %.

SOC %	x in Li_x (NiMnCo)O_2	x in LixC
0	0.70	0.050
25	0.63	0.076
50	0.54	0.093
75	0.46	0.11
100	0.38	0.12

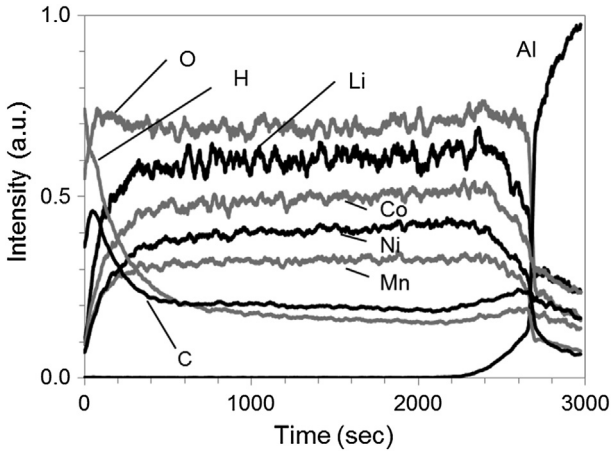

Fig. 1. GD-OES depth profile for NCM electrode with 0% SOC (The intensity ratio among the elements is not equivalent to molar ratio.).

the boundaries of the primary particles are not sharply defined and sticking mutually after measurement in Fig. 2(c). This is probably caused by the collision of Ar ions and the generation of heat in the sputtering process. However, the morphology of secondary particles of NCM remained, furthermore binder and acetylene black filling the space between the secondary particles also likely remained. This suggested that a remarkable preferential sputtering could not occur for the constituents of active material, binder, and acetylene black, and it followed by that the measured depth profile would not be distorted extremely. In the depth profile of NCM electrode (Fig. 1), however, the H and C intensities decreased with increasing depth, especially at the surface region to 500 s, though the intensities of Li, Ni, Co, Mn, and O from NMC components were homogeneous. Because preferential sputtering of the constituents was not intense on the SEM observation results, it was considered that PVdF binder and/or acetylene black were in-homogeneously distributed in depth and more of them existed in the outer layer in the NCM electrode. For more detailed investigation of the sputtered surface, XPS measurement was conducted. Fig. 3 shows XPS F1s and C1s spectra for a pristine NCM electrode sample before and after the GD-OES measurement. A strong peak at 687.8 eV in F1s spectra, which is obtained for the sample before GD-OES, is assigned to C–F of PVdF [1–3]. This peak disappeared for the sample after GD-OES measurement. The peaks at 290.8 and 286.1 eV in C1s spectra, which are assigned to C–F and C–H of PVdF [1–3], also disappeared after GD-OES measurement. Instead of those peaks, new peaks at 684.3 eV in F1s and 289.7 eV in C1s appeared after GD-OES measurement. These peaks could be assigned to Li–F and carbonate functional groups, respectively. Therefore it was suggested that some recombination products of PVdF binder and NCM could be formed on the sputtered sample surface, which would not be reflected to elemental analysis in GD-OES.

3.2. GD-OES measurement of negative electrode samples

Fig. 4 displays a GD-OES profile of Li, C, and Cu for a hard carbon electrode sample controlled to 0% SOC. Both Li and C intensities are almost constant in the middle region. The rapid increase of Cu intensity, after 4500 s, indicates that the sputtering reaches Cu current collector. The Li and C intensities are enhanced in the vicinity of the Cu current collector. This is because the sputtering rate of the sample is influenced in the presence of Cu which has a quite high sputtering yield (1.6 atoms/ion at 400 eV Ar ions [14]). The positive electrode shows a depth profile commonly seen in

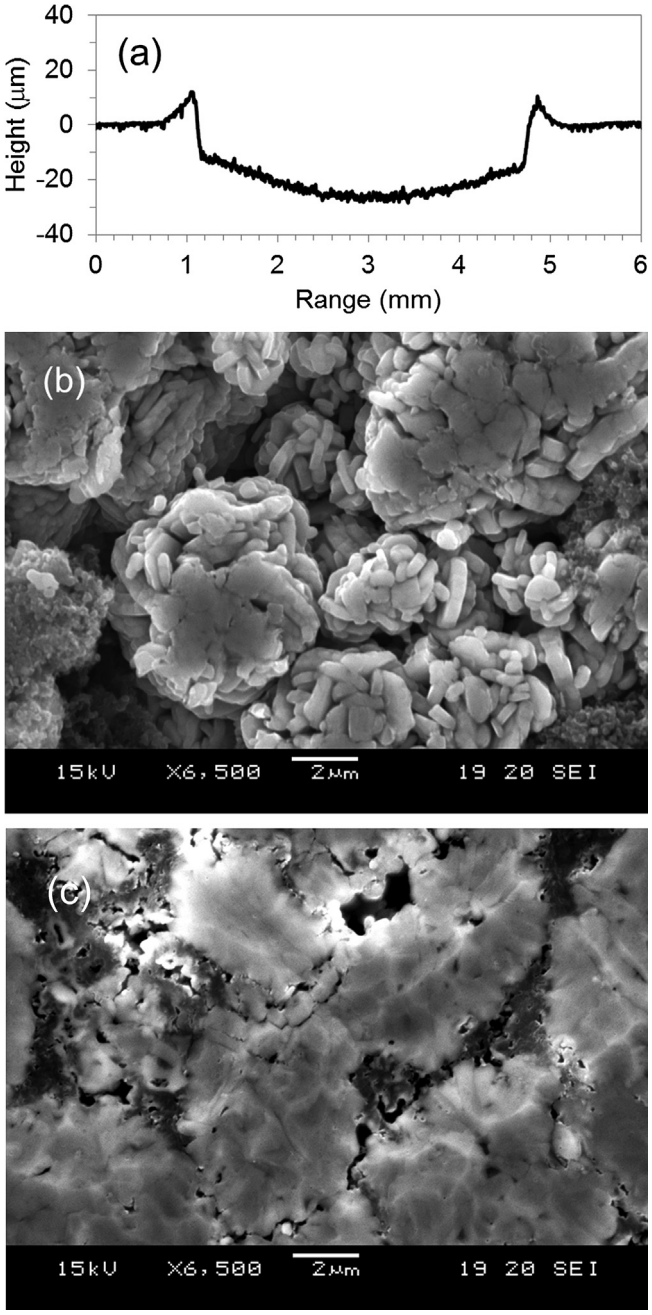

Fig. 2. Crater shape after 2000 s of GD-OES measurement (a) and SEM micrographs before (b) and after (c) 2000 s of GD-OES measurement for NCM electrode with 100% SOC.

GD-OES, where the intensities of Mn, Co, and Ni dropped down whereas the Al (0.8 atoms/ion at 400 eV Ar ions [14]) intensity increased at the interface between the electrode and the current collector (Fig. 1). In the profile of hard carbon electrode, Li and C intensities show extraordinary change at the interface of electrode layer and Cu current collector, C intensity is once drastically increased before dropping down in the vicinity of increase of Cu intensity. This might be because C and Cu have completely different characteristics in sputtering yield from each other. Fig. 5(a) and (b) shows a crater shape and a SEM micrograph for the hard carbon electrode sample with 100% SOC after 3000 s measurement. The sputtering proceeded to about 15 μm depth from the surface. The crater shape with flat bottom is mostly ideal, which is necessary for a reliable depth resolution. The sputtered surface shown in SEM

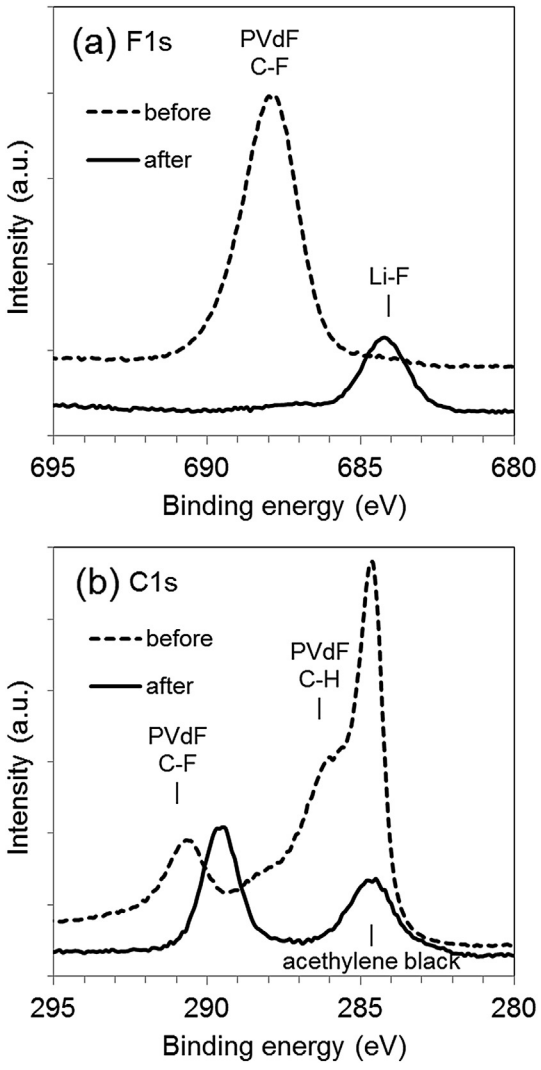

Fig. 3. F1s (a) and C1s (b) XPS spectra of a pristine NCM electrode sample before and after 2000 s of GD-OES measurement.

micrograph was smooth and the particle structure remained. These results support reliable GD-OES measurement for hard carbon electrode with SOC.

In order to understand GD-OES measurement of a carbon electrode sample deeply, the difficulty found in measuring pristine

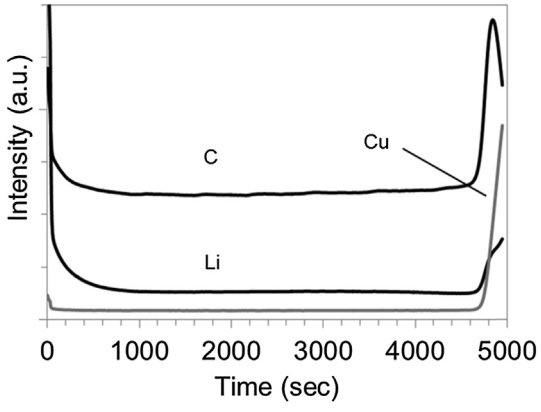

Fig. 4. GD-OES depth profile for hard carbon electrode with 0% SOC (The intensity ratio among the elements is not equivalent to molar ratio.).

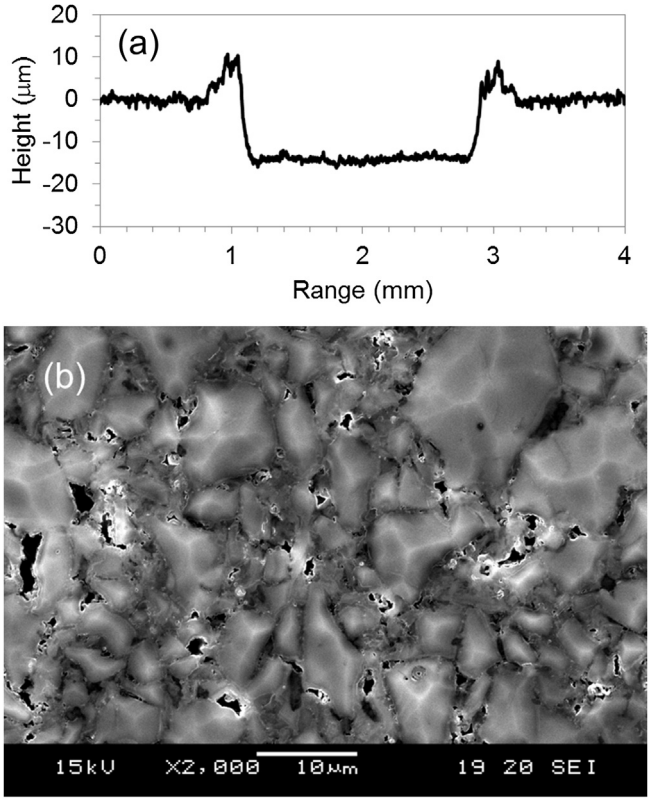

Fig. 5. Crater shape (a) and SEM micrograph (b) after 3000 s of GD-OES measurement for hard carbon electrode with 0% SOC.

hard carbon electrode should be complemented here. Fig. 6 shows a crater shape and SEM micrographs for the pristine hard carbon electrode sample before and after 3000 s measurement. The crater shape formed on the pristine hard carbon electrode shows a terribly jagged bottom in contrast to SOC sample (Fig. 5(a)). The SEM micrograph reveals that redeposited material is formed on the sputtered surface of the pristine sample, which probably brings about the rough bottom of the crater. In the depth profiling of pristine electrode, C intensity unstably decreased with sputtering time and a longer sputtering time (8000 s) was taken to reach Cu current collector (not shown). This was considered because the redeposition covering the surface area could reduce the sputtering efficiency. Fig. 7 shows F1s and C1s XPS spectra for a pristine hard carbon electrode sample before and after 3000 s of GD-OES measurement. The strong peak observed at 687.8 eV for the sample before GD-OES is assigned to C—F of PVdF. The peak at 290.8 and 286.1 eV in C1s spectra are assigned to C—F and C—H of PVdF. These peaks related to PVdF disappeared and only a peak at 284.7 eV, which is assigned to C—C in hard carbon, remains after GD-OES measurement. These results suggested that the content of PVdF binder was lower in the sputtered surface and the redeposition material was mainly composed of carbon probably maintaining hard carbon structure. Generally redeposition will happen in sputtering process; the sputtered material is returned to the sample by losing its momentum through elastic collisions in the discharge plasma. In GD-OES analysis tool, however, the gas flow is controlled in the discharge anode to lead the redeposition material to outside of the crater. Therefore the redeposition is commonly observed as a projection around the crater edge, as is shown in Fig. 5(a). It is interesting that redeposition is brought about only for a pristine carbon electrode (not only hard carbon electrode but graphite electrode), though it is suppressed for SOC samples of

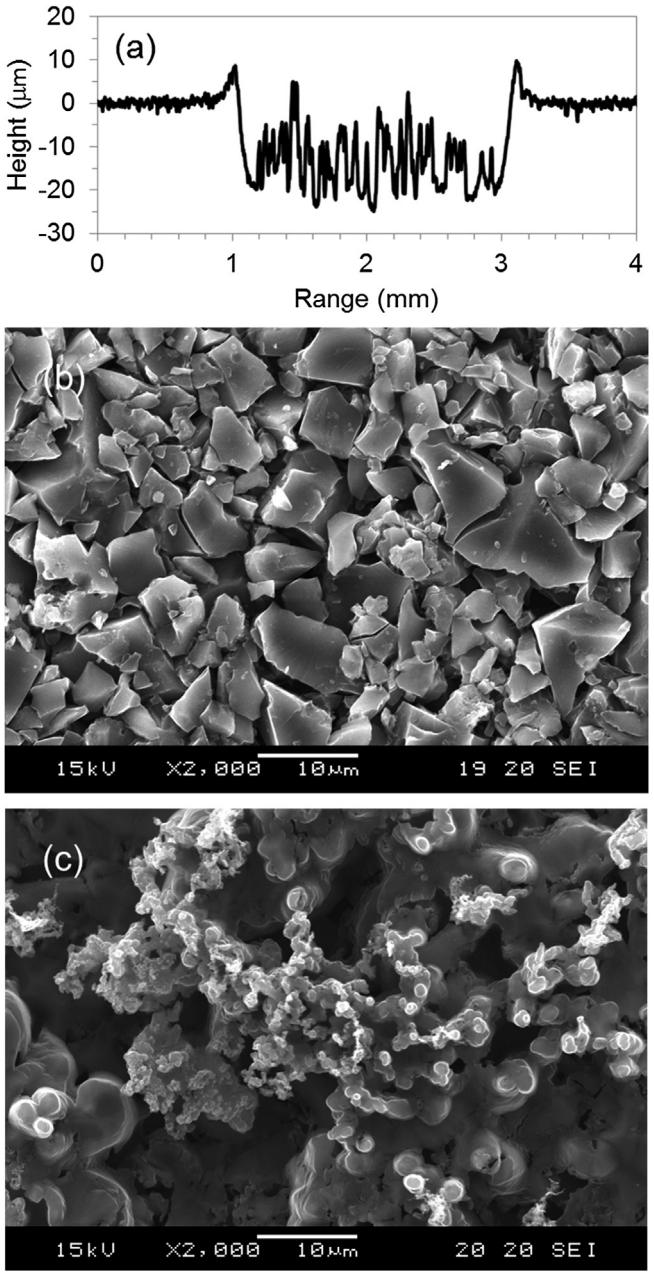

Fig. 6. Crater shape after 3000 s of GD-OES measurement (a) and SEM micrographs before (b) and after (c) 3000 s of GD-OES measurement for hard carbon electrode with 0% SOC.

them. We have also found it for neither pristine nor SOC samples of NCM and other positive electrodes such as $LiFePO_4$, $LiCoO_2$, and $LiMn_2O_4$. Further studies are needed to understand the mechanism of redeposition brought about only for a pristine carbon electrode sample.

3.3. Quantification of lithium in the electrodes

The capability of GD-OES technique for Li quantification was evaluated with use of Li intensities in the depth profiles. Fig. 8 plots Li intensities obtained from GD-OES versus Li contents by ICP-MS for the NCM electrode samples with 0–100% SOC (marked with open squares). The Li intensities were averaged from the beginning up to the inflection point of Al increment in each depth profile.

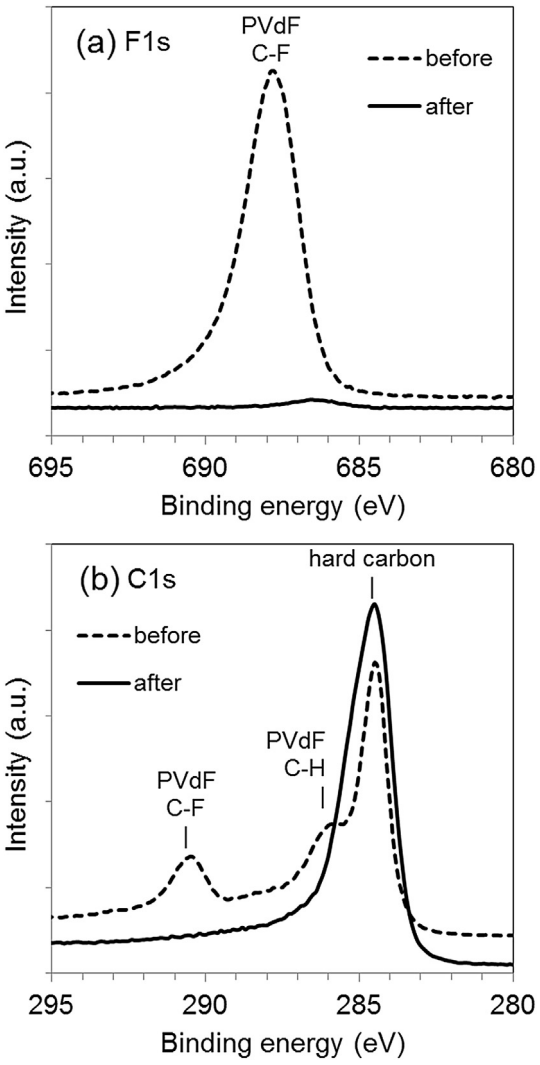

Fig. 7. F1s (a) and C1s (b) XPS spectra of a pristine hard carbon electrode sample before and after 3000 s of GD-OES measurement.

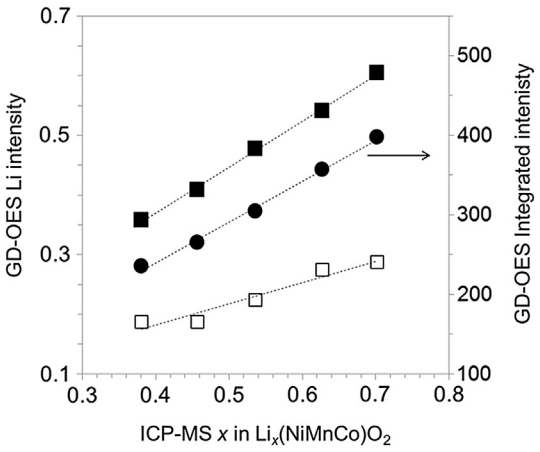

Fig. 8. Relationship between Li intensities obtained from GD-OES and Li contents determined by ICP-MS for NCM samples with 0–100% SOC. Averaged Li intensities, the intensity ratios of Li/Co, and integrated Li intensities are plotted with open squares, filled squares, and filled circles, respectively.

A linear relationship with the correlation coefficient $r^2 = 0.94$ was obtained for the averaged intensity of Li, similar to a previous report by Saito et al. [10]. In GD-OES, the emission intensity depends on the concentration of the corresponding element and the sputtering rate of the sample. Therefore, it is clear that the Li intensity can vary not only with the Li content in the sample but also with the sputtering rate of respective samples. To avoid the influence of the sputtering rate variation, the intensity ratio of Li to Co, which was one of the representative matrix elements, was recorded. The intensity ratio of Li to Co, Li/Co, versus Li contents obtained from ICP-MS is plotted with filled squares in Fig. 8. The correlation coefficient $r^2 = 0.998$ was surely improved comparing to the correlation between averaged Li intensity and ICP-MS Li contents. As an alternative mean to correct the sputtering rate variation, the integration of Li intensity was also tried. The integration of Li intensity also improved the correlation coefficient ($r^2 = 0.996$), as plotted with filled circles in Fig. 8. The reproducibilities for three time repeated measurements were 1.0% and 2.7% in the intensity ratio Li/Co and integrated Li intensity, respectively, for 75% SOC samples, whereas it was 6.6% in averaged Li intensity. By use of the calibration curve with the intensity ratio of Li/Co, which gave the best result in correlation coefficient and reproducibility, the depth profiles of Li were quantified for the NCM electrode samples with 0–100% SOC (Fig. 9). The Li contents in the middle region of profiles are constant in depth and trend to decrease with increasing SOC. At the surface region, it was found that Li contents decreased for 50–100% SOC samples. This suggested that Li contents were low at the surface of highly charged state over 50% of the NCM electrode samples.

Similarly, the Li quantification by GD-OES was evaluated for the hard carbon electrode samples. Fig. 10 plots Li intensities obtained from GD-OES versus Li contents by ICP-MS for the samples with 0–100% SOC, marked with open squares. The Li intensities were taken average from the beginning up to the inflection point of Cu increment for each data. A good linear relationship was obtained, and the correlation coefficient was $r^2 = 0.97$. Either intensity ratio of Li to C as a matrix element, Li/C, or integration of Li intensity improved the correlation coefficient of the relationship with ICP-MS Li contents ($r^2 = 0.98$), which were plotted with filled squares and filled circles, respectively, in Fig. 10. The reproducibilities for three time repeated measurements were 2.0% and 2.7% in the intensity ratio Li/C and integrated Li intensity, respectively, for 75% SOC samples, whereas it was 3.7% in averaged Li intensity. Recording intensity ratio of Li/C would enable the most reliable quantification of Li in hard carbon electrode from the points of correlation in the calibration curve and reproducibility. Fig. 11

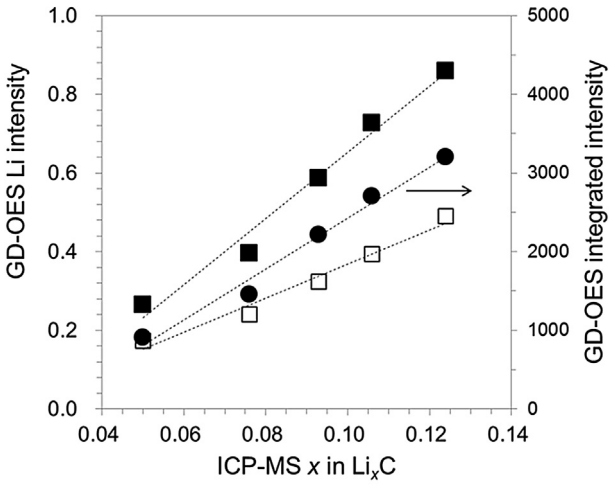

Fig. 10. Relationship between Li intensities obtained from GD-OES and Li contents determined by ICP-MS for hard carbon electrode samples with 0–100% SOC. Averaged Li intensities, the intensity ratios of Li/C, and integrated Li intensities are plotted with open squares, filled squares, and filled circles, respectively.

shows Li depth profiles for the hard carbon electrode samples with 0–100% SOC quantified with the Li/C calibration curve. The contents in the middle region of profiles tend to increase with increasing SOC %. At the top surface region, high contents of Li were observed for all samples. This top surface peak could be attributed to the deposition formed on the negative electrode surface, which is called SEI. The variation in surface profile showed that the thickness of the surface deposition was increased for highly charged states of the electrode samples. Recently depth profile of SEI film on graphite electrode surface was investigated using photoelectron spectroscopy (PES) [15]. The results indicate that the SEI of charged negative electrode is thicker than that of discharged one, since the PES graphite peak does not appear until bulk sensitive measurement at high kinetic energy for the charged electrode. The thickness variation of the surface deposition shown in GD-OES profiles might agree with the PES study. Except for the top surface region, Li content was almost constant for 0% SOC electrode, which suggested homogeneous distribution of Li in the electrode. In contrast, Li contents gradually decreased in depth for the electrodes from 25 to 100% SOC. It likely appeared that the decreasing slope was high for 75% SOC especially. These suggested that large amount of Li was present in the outer layer and inhomogeneous distribution

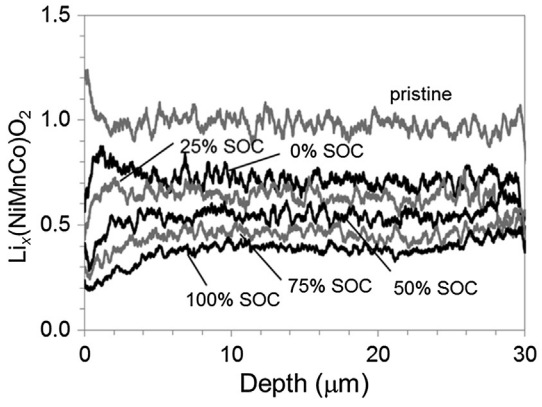

Fig. 9. Depth profiles of Li for NCM samples with 0–100% SOC which were quantified with the calibration curve using Li/Co intensity ratio, shown in Fig. 8.

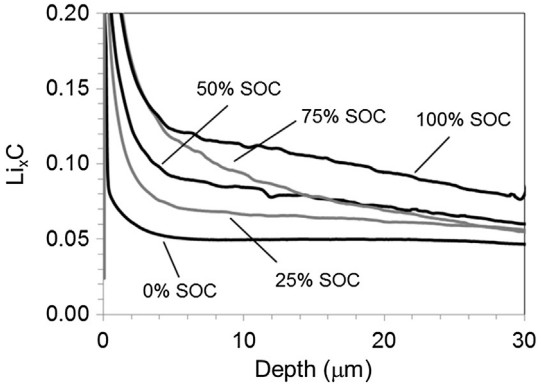

Fig. 11. Depth profiles of Li for hard carbon samples with 0–100% SOC which were quantified with the calibration curve using GD-OES Li/C intensity ratio, shown in Fig. 10.

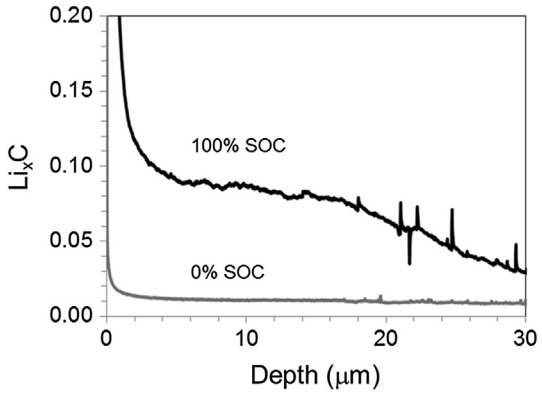

Fig. 12. Depth profiles of Li for graphite electrode samples with 0 and 100% SOC. Li compositions determined by ICP-MS are respectively $x = 0.021$ and 0.12 in Li_xC.

of Li happened in the electrodes with highly charged state. We examined separately the possibility of preferential sputtering of Li over C which can be responsible for the decreasing slope in the depth profiles. For a graphite electrode with a certain amount of Li_3PO_4, which was prepared by mixing the chemical regent in the composite slurry, the depth profile exhibited almost constant concentration of Li in whole electrode region (not shown). Therefore it was concluded that no apparent preferential sputtering of Li over C could occur in GD-OES and the Li profile for the 25–100% SOC suggested inhomogeneous distribution of Li in depth. We also attempted to evaluate a few graphite electrode samples which were set to 0 and 100% SOCs for references (Fig. 12). The results showed that Li was homogeneously present in the graphite electrode with 0% SOC similarly to the corresponding hard carbon electrode sample. For 100% SOC sample, however, it was suggested that Li content was almost constant in the outer layer and abruptly decreased in the inner layer.

4. Conclusion

GD-OES analysis technique was applied to NCM and hard carbon electrodes with 0–100% range of SOC. The NCM positive electrode samples were measured in depth from the surface to the Al current collector around 2000–3000 s. The hard carbon electrodes were also successfully measured up to the Cu current collector, though it took longer time than the positive electrode, 5000–8000 s, because of the low sputtering yield of carbon. The crater shapes were flat, whereas slightly concave at the edge for NCM samples, suggesting a good depth resolution in the profiles for both positive and negative electrodes. SEM images show the electrode surfaces after the GD-OES measurement were smooth and traceable to the original form, suggesting that remarkable preferential sputtering of the composite materials does not occur for the samples. Only for pristine hard carbon electrode sample, redeposition during sputtering process was observed. The GD-OES intensity of Li was linearly correlated to the Li components determined by ICP-MS for the positive and negative electrode samples. The correlation coefficients of the linear relationship were improved when the intensities were corrected on sputtering rate by taking intensity ratio of the Li to the intensity of matrix element, Li/Co and Li/C for NCM and hard carbon electrodes, respectively, or by integrating Li intensity.

Acknowledgments

We are grateful to Dr. Hikari Sakaebe (AIST), Professor Tatsuya Nakamura (University of Hyogo), and Dr. Yo Kobayashi and Dr. Takeshi Kobayashi (CRIEPI) for their technical help and comments. We would also like to thank Atsushi Kojyo, Dr. Kenji Kodama and Noboru Yamashita (Rigaku Corp.) and Michael Analytis and Rudiger Meihsner (SPECTRUMA Analytik Gmbh) for their technical support on GD-OES measurements.

References

[1] A.M. Andersson, D.P. Abraham, R. Haasch, S. MacLaren, J. Liu, K. Amine, J. Electrochem. Soc. 149 (2002) A1358.
[2] R. Dedryvere, S. Laruelle, S. Grugeon, L. Gireaud, J.-M. Tarascon, D. Gonbeau, J. Electrochem. Soc. 154 (2005) A689.
[3] M. Shikano, H. Kobayashi, S. Koike, H. Sakaebe, E. Ikegawa, K. Kobayashi, K. Tatsumi, J. Power Sources 174 (2007) 795.
[4] B.M. Meyer, N. Leifer, S. Sakamoto, S.G. Greenbaum, C.P. Grey, Electrochem. Solid-State Lett. 8 (2005) A145.
[5] Y. Wang, V. Yufit, X. Guo, E. Peled, S. Greenbaum, J. Power Sources 94 (2001) 230.
[6] Z. Wang, N. Dupre, L. Lajaunie, P. Moreau, J.-F. Martin, L. Boutafa, S. Patoux, D. Guyomard, J. Power Sources 215 (2012) 170.
[7] J. Kikkawa, T. Akita, M. Tabuchi, K. Tatsumi, M. Kohyama, Electrochem. Solid-State Lett. 11 (2008) A183.
[8] R.K. Marcus (Ed.), Glow Discharge Spectroscopies (Modern Analytical Chemistry), Plenum Pub Corp, New York, 1993, p. 128.
[9] M. Winchester, R. Payling, Spectrochim. Acta, Part B 59 (2004) 607.
[10] Y. Saito, M.K. Rahman, J. Power Sources 174 (2007) 877.
[11] Masahiro Shikano, Hironori Kobayashi, Shinji Koike, Hikari Sakaebe, Yoshiyasu Saito, Hironobu Hori, Hiroyuki Kageyama, Kuniaki Tatsumi, J. Power Sources 196 (2011) 6881.
[12] H. Kobayashi, Y. Arachi, S. Emura, H. Kageyama, K. Tatsumi, T. Kamiyama, J. Power Sources 146 (2005) 640.
[13] T. Neils, R. Payling (Eds.), Glow Discharge Optical Emission Spectroscopy: A Practical Guide, The Royal Society of Chemistry, Cambridge, 2003, pp. 40–43.
[14] R.K. Marcus (Ed.), Glow Discharge Spectroscopies (Modern Analytical Chemistry), Plenum Pub Corp, New York, 1993, pp. 30–31.
[15] S. Malmgren, H. Rensmo, T. Gustafsson, M. Gorgoi, K. Edstrom, Electrochem. Soc. Trans. 25 (36) (2010) 201.